



Article

Treatment of Shale Gas Flowback Wastewater by Electroflocculation Combined with Peroxymonosulfate

Yuanjie Liang¹, Xia Li¹, Qi Feng^{2,*} , Mohamed Gamal El-Din³ , Pamela Chelme-Ayala³ and Longjun Xu^{2,*}

¹ Chongqing Vocational Institute of Safety Technology, Chongqing 404020, China; yuanjieliang2024@163.com (Y.L.); liang_keyan@163.com (X.L.)

² State Key Laboratory of Coal Mine Disaster Dynamics and Control, Chongqing University, Chongqing 400044, China

³ Department of Civil and Environmental Engineering, University of Alberta, Edmonton, AB T6G 1H9, Canada; mgamalel-din@ualberta.ca (M.G.E.-D.); chelmeayala@ualberta.ca (P.C.-A.)

* Correspondence: qifeng868@cqu.edu.cn (Q.F.); xulj@cqu.edu.cn (L.X.)

Abstract: In this study, potassium peroxymonosulfate was added to an electrolytic cell with an iron anode to achieve the dual flocculation and sulfate-radical-driven oxidative degradation of organic matter in shale gas flowback wastewater. The effects of current density, solution pH, and potassium peroxymonosulfate concentration on organic matter degradation were investigated. The results showed that chemical oxygen demand (COD) removal reached 93.4% at a current density of 40 mA/cm², pH 7, and a potassium peroxymonosulfate concentration of 1500 mg/L, surpassing the efficiency of single electroflocculation (82.4%). The characterization of the coupled electroflocculation and peroxymonosulfate system confirmed the production of sulfate radicals and identified Fe₂O₃ as the primary final product in the treated wastewater. The introduction of sulfate significantly enhanced organic matter degradation, accelerated the reaction rate and improved the overall efficiency of the treatment process. This study offers valuable insights into the chemical synergistic treatment approach and its potential applications in organic wastewater treatment.

Keywords: electroflocculation; potassium peroxymonosulfate; oxidation; sulfate radical; shale gas flowback wastewater



Academic Editor: Enric Brillas

Received: 9 October 2024

Revised: 9 December 2024

Accepted: 13 December 2024

Published: 31 December 2024

Citation: Liang, Y.; Li, X.; Feng, Q.; El-Din, M.G.; Chelme-Ayala, P.; Xu, L. Treatment of Shale Gas Flowback Wastewater by Electroflocculation Combined with Peroxymonosulfate. *Catalysts* **2025**, *15*, 28. <https://doi.org/10.3390/catal15010028>

Copyright: © 2024 by the authors. Licensee MDPI, Basel, Switzerland. This article is an open access article distributed under the terms and conditions of the Creative Commons Attribution (CC BY) license (<https://creativecommons.org/licenses/by/4.0/>).

1. Introduction

Hydraulic fracturing is a cornerstone technique in shale gas extraction, that is widely applied across the industry [1]. However, this practice raises substantial environmental concerns, primarily due to the diverse array of chemical additives in fracturing fluids. These chemicals create flowback wastewater containing a complex mixture of organic compounds and heavy metals, which poses significant challenges for effective decomposition [2]. This contamination is characterized by elevated levels of chemical oxygen demand (COD), dissolved solids, and salinity, as well as significant changes in the coloration of the flowback fluid [3]. The toxic-laden shale gas flowback wastewater is distinct from municipal or industrial wastewater and poses serious risks to human health, animal well-being, and ecological balance [4]. Deep-ground injection wells constituted the main method for managing shale gas wastewater which mainly involved the construction of disposal wells, which inherently carry significant environmental risks [1,5]. Modern degradation methods, such as membrane-based processes, biological treatment, and electrochemical oxidation, offer alternatives but are not without challenges. These methods face issues such as

insufficient treatment efficiency, high operational costs, and equipment corrosion, limiting their widespread application [6,7]. Given these challenges, there is an undeniable urgency to mitigate environmental impacts, necessitating the exploration and adoption of more sustainable and less hazardous treatment methods.

Electroflocculation, known for its environmental sustainability and effectiveness in water purification, operates through anodic dissolution. This process catalyzes the hydrolytic generation of abundant cations, which subsequently form complexes that aid in removing suspended particulates from wastewater through entrapment and adsorption. [8,9]. Characterized by its potent pollutant adsorption capacity, this method boasts high treatment efficiency, cost-effectiveness, and the absence of secondary pollution, positioning it as a superior alternative within the water treatment spectrum [10,11]. Its application extends across various domains, including the remediation of oily wastewater and industrial effluents, underscoring its versatility and wide acceptance in contemporary environmental management practices. Kausley [12] applied electroflocculation to treat oilfield fracturing wastewater, effectively removing total organic carbon and reducing water hardness. The study examined the effects of formulated high-concentration salt-containing return wastewater, low-concentration return wastewater, and the original actual wastewater on treatment efficiency and energy consumption. The results indicated that higher electrical conductivity led to increased energy consumption and a more significant flocculation effect. Gao [13] compared the treatment of uranium-containing wastewater using traditional flocculation and electroflocculation. The study found that both methods efficiently removed uranium; however, electroflocculation offered easier automation control, lower treatment costs, and less floc generation, suggesting it has better prospects for widespread application. Franco [14] used electroflocculation to remove phosphate from groundwater and investigated the effects of initial conductivity, power supply, and initial pH on phosphorus removal efficiency. The results showed that higher conductivity increased energy consumption and improved the flocculation effect, achieving up to 99% phosphorus removal within a pH range of 5.5–8. Verma [15] employed an electroflocculation process with Fe-Al composite electrodes to treat textile wastewater, achieving more than 90% COD removal and chromaticity under optimized conditions. Ma [16] conducted an experimental study on treating polysulfur mud system drilling wastewater using electroflocculation, reporting a COD removal rate of 94.2% after 75 min of treatment. However, the electroflocculation method has certain limitations, such as lower electrode efficiency and high energy consumption [17]. As a result, enhancing process stability and ensuring long-term efficient operation have become key research focuses.

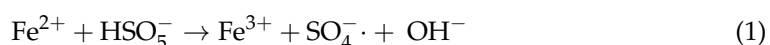
The utilization of activated persulfate or peroxymonosulfate to generate sulfate radicals for the degradation of organic contaminants in industrial wastewater, groundwater, and soil represents an innovative approach that has recently gained recognition [18,19]. This technique involves the activation of persulfate using transition metals or their ions (such as Fe, Fe²⁺, Ag⁺, Cu²⁺, Mn²⁺, etc.), and has emerged as a promising solution for environmental remediation. Distinguished by its effectiveness in targeting a broad spectrum of organic pollutants, this method offers a novel pathway for mitigating environmental pollution challenges associated with industrial activities and contamination in various matrices. Li et al. [20] explored the dual role of an annular iron sheet as both an electrode and an activator source, combined with electrolysis techniques, for activating persulfate or peroxymonosulfate to enhance the degradation of dinitrodiazophenol in an aqueous solution. However, this system faces drawbacks such as prolonged operation time, low persulfate oxidation efficiency, and limited utilization rate.

This study integrated potassium peroxymonosulfate into the electroflocculation process for treating shale gas flowback wastewater, aiming to overcome the limitations asso-

ciated with using electroflocculation and transition metal-activated peroxymonosulfate oxidation independently. The objective was to achieve a synergistic effect between flocculation and oxidative degradation, thereby enhancing the efficiency of wastewater treatment. Our research focuses on elucidating the degradation mechanism and reaction kinetics by analyzing the final flocculate, providing a theoretical foundation for further exploration of the combined approach of electroflocculation and persulfate oxidation in wastewater remediation.

2. Results and Discussion

The optimum parameters for the electroflocculation treatment of shale gas flowback wastewater were established through a series of single-variable experiments, resulting in a current density of 30 mA/cm², an inter-electrode distance of 2 cm, and a solution pH of 8.5. Within this operational framework, the COD removal efficiency achieved was 82.4%, accompanied by a reduction in the mass of iron electrodes by 0.1058 g. Especially, the potassium peroxymonosulfate triple salt typically consists of the following proportions by weight: KHSO₅ (42.8%), KHSO₄ (~22.0%), and K₂SO₄ (~35.2%). According to Equation (1) and accounting for the proportion of KHSO₅ in the potassium peroxymonosulfate complex, an initial concentration of potassium peroxymonosulfate of about 1200 mg/L was chosen for further optimization.

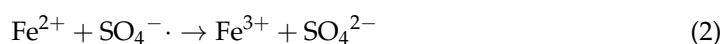


2.1. Process Optimization of Collaborative Wastewater Treatment

2.1.1. Influence of Current Density on COD Removal Rate

Elevating the current density in the electroflocculation process enhances floc formation and hydrogen production, thus increasing the method's efficiency. However, excessively high current densities can cause electrode polarization and form a passivation layer, which may reduce the process's effectiveness. Given the significant impact of current density on electroflocculation performance, careful regulation is essential.

This study investigated the effects of current densities ranging from 10 to 50 mA/cm² on the degradation efficiency of shale gas flowback wastewater using an electroflocculation system combined with potassium peroxymonosulfate. As shown in Figure 1, the optimal removal efficiency of 70.3% was achieved at a current density of 40 mA/cm². This peak efficiency resulted from the increased rate of Fe²⁺ generation at higher current densities, significantly improving flocculation. Additionally, the activation of potassium peroxymonosulfate boosted the production of sulfate radicals, further aiding in the degradation of organic compounds in the wastewater. However, when the current density exceeded 40 mA/cm², the removal efficiency decreased. This decline is due to the adverse effects of high current densities on the flocculation process, which diminished its effectiveness. Moreover, the rapid generation of Fe²⁺ at higher concentrations led to its quick interaction with sulfate radicals (as described in Equation (2)), resulting in the rapid depletion of these radicals and a subsequent reduction in the system's degradation capacity. Consequently, the experiment proceeded with an optimal 40 mA/cm² current density.



2.1.2. Influence of pH on COD Removal Rate

The efficacy of the electroflocculation process is significantly influenced by the solution's pH, as it affects the production of hydrogen and oxygen species [21]. As shown in Figure 2, the pH plays a crucial role in the combined treatment of shale gas flowback wastewater using electroflocculation and potassium peroxymonosulfate. COD removal

efficiency improves with increasing the pH to 7, where the maximum COD removal rate reaches 85.2%. This optimal performance is primarily due to the favorable dissolution rate of iron under these conditions, which promotes the formation of sulfate radicals. In more acidic environments, the accelerated fragmentation of peroxydisulfate leads to higher concentrations of sulfate radicals [22,23]. However, this increase also triggers more frequent quenching reactions among free radicals, reducing their availability to react with organic pollutants. With increasing the pH to 8.5, Fe^{2+} primarily exists as $\text{Fe}(\text{OH})_2$, $\text{Fe}(\text{OH})_3$ (as shown in the Equation (3)), and other hydrolyzed products, reducing the effective activation of PMS by Fe^{2+} and the generation of reactive species. In mildly alkaline conditions, OH^- ions compete with pollutants for reactive radicals [24,25], resulting in a decrease in COD removal efficiency. The results demonstrate that a pH of 7 is the most conducive to achieving the highest efficacy in this synergistic treatment approach.

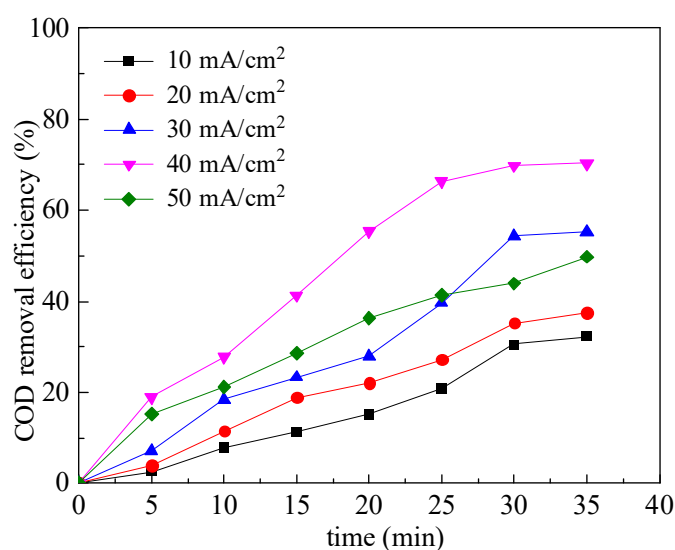


Figure 1. Effect of time on COD removal at different current densities.

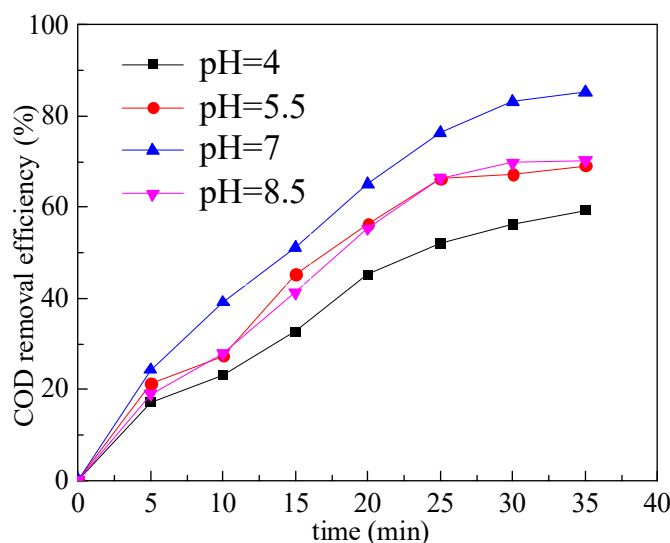


Figure 2. Effect of time on COD removal at different pH values.

2.1.3. Influence of Potassium Peroxymonosulfate Concentration on COD Removal Rate

The degradation of organic compounds via sulfate-radical-mediated pathways involves three fundamental mechanisms: hydrogen abstraction, electron transfer, and ad-

dition across double bonds [26]. The effect of varying potassium peroxydisulfate concentrations on wastewater treatment efficiency, ranging from 900 to 2100 mg/L, are illustrated in Figure 3. The data show an initial positive relationship between the peroxydisulfate concentration and removal efficiency. At a potassium peroxydisulfate concentration of 1500 mg/L, the removal rates for COD and TOC reached their maximum values of 93.4% and 86.7%, respectively, with a conductivity of 27.8 mS/cm. These results are likely attributable to the reactions occurring during electrocoagulation coupled with PMS activation, as described by Equations (1) and (4)–(6) [27,28]. However, beyond this concentration, the treatment effectiveness began to decline. This decrease is primarily due to the excessive reaction between sulfate radicals and sulfate ions or other sulfate radicals as shown in the Equations (7) and (8), which reduced the utilization rate of sulfate radicals and, consequently, the system's ability to treat organic pollutants in wastewater [29]. Therefore, a concentration of 1500 mg/L for potassium peroxydisulfate was selected for subsequent experiments, balancing treatment efficacy with economic feasibility.

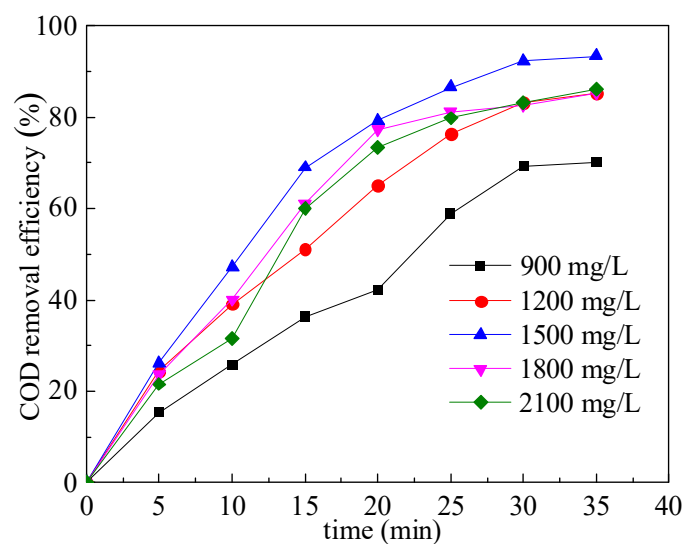
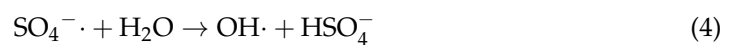
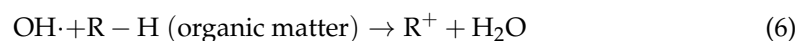
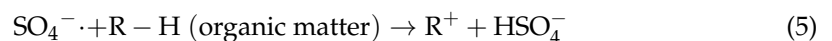


Figure 3. Effect of time on COD removal at different potassium peroxydisulfate concentrations.



2.2. Preliminary Kinetic Analysis

2.2.1. Influence of Current Density on Reaction Parameters

The relationship between $\ln(\text{COD}_0/\text{COD}_t)$ and time, and the corresponding fitting parameters under different current densities, are illustrated in Figure 4 and Table 1 respectively. The experiment conditions were the same as Section 2.1.1. It can be observed from the figure that linear fitting curves were obtained consistently across various current densities. The observed results indicate that the collaborative wastewater treatment adheres to the first-order reaction kinetics model, with the slope of the fitting curve representing the reaction rate (r). It can be observed from the graph that as current density increases, the

r value rises from 0.0177 to 0.0380. However, at a current density of 50 mA/cm², there is a decrease in the r value to 0.0187 due to elevated sulfate radical concentration inhibiting its activity and subsequently reducing the reaction rate.

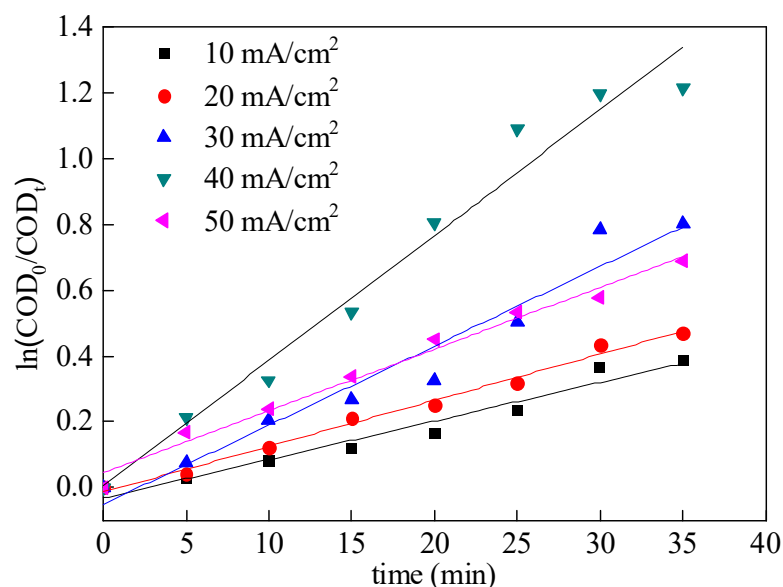


Figure 4. Time to kinetic fitting equations at different current densities (COD₀ is the initial concentration of COD, COD_t is the COD concentration at some point).

Table 1. Time to kinetic fitting parameters at different current densities.

Current Density (mA/cm ²)	Kinetic Reaction Equations	Reaction Rate (min ⁻¹)	R ²
10	$\frac{\ln \text{COD}_0}{\ln \text{COD}_t} = 0.0117t - 0.0324$	0.0117	0.957
20	$\frac{\ln \text{COD}_0}{\ln \text{COD}_t} = 0.0140t - 0.0147$	0.0140	0.988
30	$\frac{\ln \text{COD}_0}{\ln \text{COD}_t} = 0.0241t - 0.0519$	0.0241	0.936
40	$\frac{\ln \text{COD}_0}{\ln \text{COD}_t} = 0.0380t + 0.0540$	0.0380	0.968
50	$\frac{\ln \text{COD}_0}{\ln \text{COD}_t} = 0.0187t + 0.0454$	0.0187	0.994

2.2.2. Preliminary Kinetic Analysis Under Optimal Conditions of Electroflocculation and Cooperative Treatment

The kinetic analysis of the combined electroflocculation and potassium peroxymonosulfate treatment of flowback wastewater under optimal conditions is represented in Figure 5. This analysis demonstrates that including potassium peroxymonosulfate does not modify the kinetic order of the electroflocculation process, with both treatments adhering to first-order kinetics. The relevant kinetic equations and parameters are detailed in Table 2. The addition of potassium peroxymonosulfate enhances the rate constant from 0.0575 to 0.0860, signifying not only the generation of sulfate radicals but also their efficacy in expediting the breakdown of organic contaminants into smaller molecules, including organic acids, through electrochemical reactions. Moreover, these processes potentially lead to the further oxidation of such molecules into carbon dioxide and water, highlighting the efficiency of potassium peroxymonosulfate in augmenting the degradation capabilities of the electroflocculation treatment.

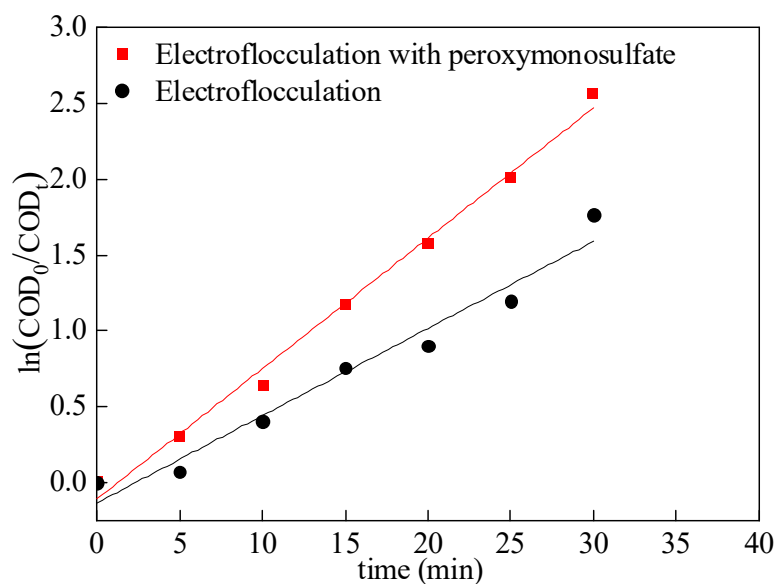


Figure 5. Coordination and electroflocculation dynamics fitting equation.

Table 2. Coordination and electroflocculation fitting parameters of synergism and electroflocculation kinetics.

	Fitting Equation	Reaction Rate (min ⁻¹)	R ²
Electroflocculation with peroxymonosulfate	$\frac{\ln \text{COD}_0}{\ln \text{COD}_t} = 0.0860t - 0.1092$	0.0860	0.992
Electroflocculation	$\frac{\ln \text{COD}_0}{\ln \text{COD}_t} = 0.0575t - 0.135$	0.0575	0.959

2.3. Characterization of Flocculation Products and Electrochemical Analysis

2.3.1. XRD Patterns of Flocculation Products

The XRD diffraction patterns (Figure 6) of the flocculated products show a mixture of broad and narrow peaks. The presence of these peaks suggests that multiple phases may exist within the sample or that there could be contributions from non-crystalline or amorphous materials. A comparison with the standard card (JCPDS 76-1821) reveals that the dominant crystal planes at (015), (202), and (123) correspond to the characteristic diffraction peaks of hexagonal Fe₂O₃. The peak intensity observed for the collaborative treatment is significantly enhanced compared to that for the conventional flocculation method, resulting in sharper peaks. This enhancement indicates an improvement in the crystallinity of nano-Fe₂O₃ [29]. The diffraction peaks at 38.5° and 70.6° observed in the XRD patterns may correspond to secondary phases or impurities. Based on Crystallography Open Database database matching, these peaks align well with SnO₂ (2θ = 38.3°, 70.6°) and less strongly with Fe₂S₄, which suggests that these peaks might originate from different phases or experimental artifacts, such as reflections from the sample holder or residual salts present in the treated wastewater. Moreover, experimental artifacts such as reflections from the sample holder or residual salts (e.g., K₂SO₄ or FeSO₄) may contribute to these peaks. The addition of potassium peroxymonosulfate almost does not alter the primary flocculation products during the treatment of electroflocculated wastewater. The resulting sludge primarily comprises iron and ferrous polyhydroxyl polymers, with Fe₂O₃ being generated through dehydration.

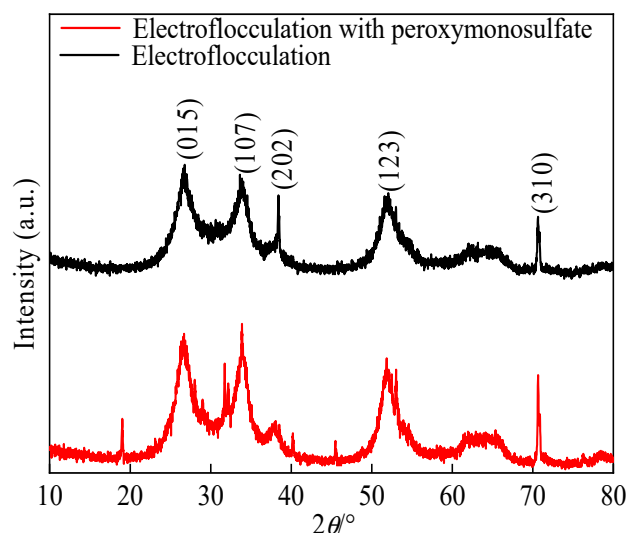


Figure 6. XRD spectrum of flocculated product.

Based on the half-peak width of the three main crystal faces (015), (107), and (123), the average crystallite size of Fe_2O_3 is calculated using the Debye-Scherrer Equation (9). After electroflocculation treatment, the crystallite size is 69.1 nm, while after collaborative treatment, it decreases to 61.6 nm. This reduction suggests that adding potassium peroxymonosulfate effectively activates the process and inhibits organic matter degradation by sulfate radicals, thereby limiting the growth of Fe_2O_3 crystallites [29]. Additionally, these narrow peaks of electroflocculation with peroxymonosulfate likely arise from secondary phases or impurities introduced during the experimental process. Potential explanations include: (1) the collaborative treatment may have induced the formation of small amounts of secondary phases with higher crystallinity compared to the primary phase of Fe_2O_3 . These phases could include oxides, sulfates, or hydroxides formed due to the interaction between potassium peroxymonosulfate and other ions in the solution [30]. (2) Narrow peaks might correspond to unreacted salts or byproducts from the reaction, such as crystallized compounds.

$$D_{hkl} = \frac{0.89\lambda}{B\cos\theta} \quad (9)$$

Here, D_{hkl} is the crystallite size (nm), λ is the X-ray wavelength (0.154 nm), B is the half-peak width (rad), and θ is the diffraction angle ($^\circ$).

2.3.2. FT-IR Spectra of Flocculation Products

The FT-IR analysis of the flocculation products, as illustrated in Figure 7, reveals the distinct absorption frequencies of infrared light, which elucidate the presence of various chemical bonds and functional groups within the spectrum. Notably, the electroflocculation process, both independently and in conjunction with potassium peroxymonosulfate treatment, shows considerable overlap in the absorption bands. The peaks at 3423 cm^{-1} and 3434 cm^{-1} indicate the stretching vibrations of the hydroxyl hydrogen bond (-OH), highlighting the formation of iron hydroxyl complexes in the flocculation products. Similarly, the absorption peaks at 1654 cm^{-1} and 1632 cm^{-1} are attributed to the water-associated -OH groups. The vibrational spectral bands corresponding to the Fe-O bonds in hematite are identified at 607 cm^{-1} and 621 cm^{-1} . These results suggest that the flocculation products derived from treating flowback wastewater via electroflocculation, either alone or in combination with potassium peroxymonosulfate, are primarily composed of iron oxides and bound water molecules, with dehydration processes converting these complexes to Fe_2O_3 as a predominant end product. Furthermore, the FT-IR spectra from the combined

treatment method reveal the presence of strong S=O stretching vibrations at 1195 cm^{-1} and 1109 cm^{-1} , which were not observed in the electroflocculation products. This difference may be explained by the interaction between the complexing agents and sulfate radicals in the solution, or possibly the result of redox reactions between sulfate radicals and organic compounds in the electroflocculation with the peroxymonosulfate system. This underscores the enhanced reactive pathways facilitated by the addition of potassium peroxymonosulfate in the treatment process, leading to a distinct chemical signature in the flocculation products.

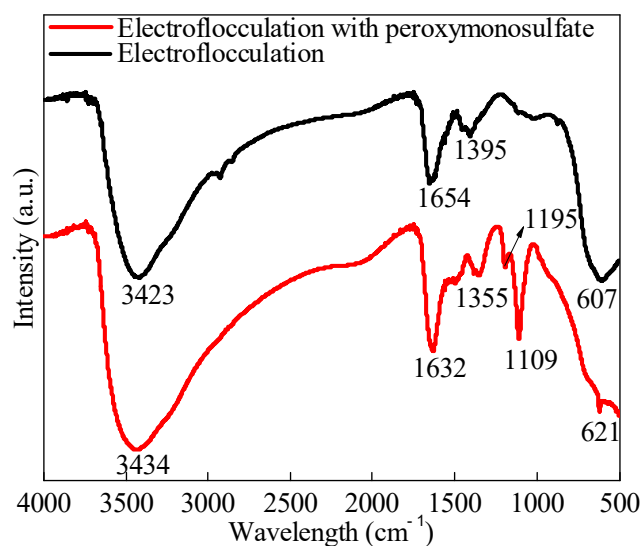


Figure 7. FT-IR spectrum of flocculation product.

2.3.3. SEM of Flocculation Products

Figure 8 presents the SEM images of flocculated products. The surface products in Figure 8a display an uneven and disordered distribution. At a magnification of $1000\times$, irregular particles with predominantly mesoporous dimensions are observed, which seem to contribute to the agglomeration of the flocculates [31]. This observation suggests that the flocculation process involves the incorporation of non-degraded polymeric organic matter. In contrast, the surface of the product in Figure 8b exhibits a rough and fluffy texture, with a relatively uniform distribution of the flocculated product. Fine particles adorn the surface, indicating that the polymeric organic matter in the wastewater has been effectively degraded and adsorbed by the floc [32]. This observation highlights the strong adsorption and sweeping capabilities of the floc.

2.3.4. EDS Element Analysis

The EDS analysis of flocculation products, as shown in Figure 9 and detailed in Table 3, reveals the elemental composition of flocculates derived from both individual electroflocculation and its combined application with peroxymonosulfate. The analysis indicates the predominance of elements such as oxygen (O), sodium (Na), sulfur (S), chlorine (Cl), and iron (Fe) within the flocculates. In particular, the flocculates obtained from electroflocculation alone show iron (Fe) and oxygen (O) as the major components, with atomic percentages of 36.72% and 59.87%, respectively. These proportions peak in the flocculates from the combined method, highlighting the enhanced efficiency of the synergistic approach. A distinctive characteristic of the flocculates from the combined treatment, compared to electroflocculation alone, is the presence of sulfur (S), suggesting the involvement of sulfate radicals in the flocculation process due to peroxymonosulfate activation. The atomic S ratio is approximately 1:4, reflecting the oxidative dynamics

facilitated by sulfate radicals during treatment. Additionally, trace amounts of Na^+ and Cl^- ions were observed, likely remnants of the high salinity characteristic of the wastewater being treated. These ions are encapsulated within the flocculation products, indicating the complex nature of the treatment matrix and the comprehensive removal capabilities of the combined electroflocculation and peroxymonosulfate method.

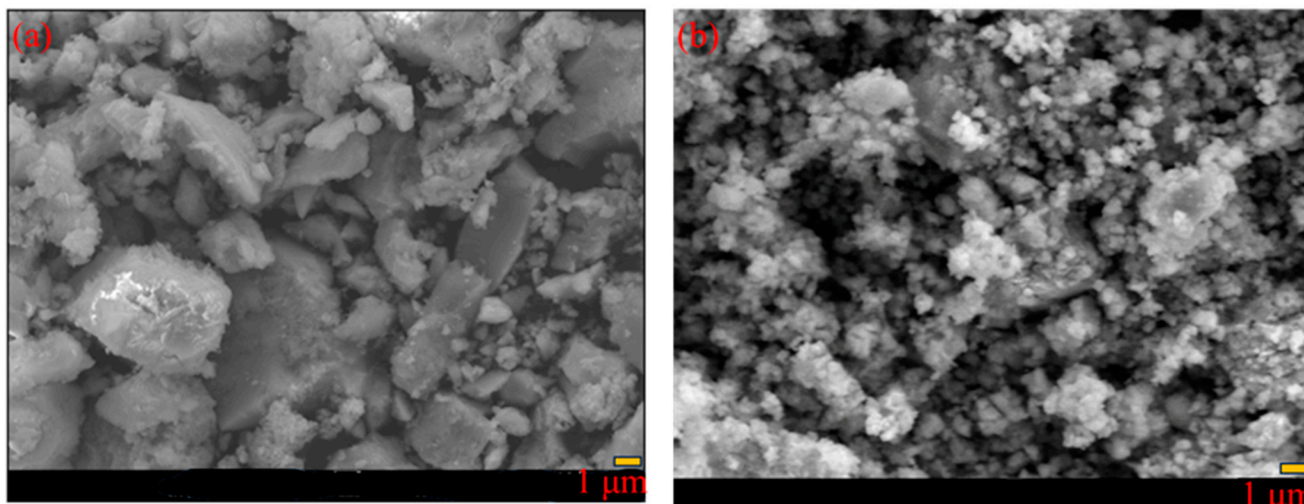


Figure 8. SEM spectrum of flocculation product: (a) electroflocculation; (b) electroflocculation with peroxymonosulfate.

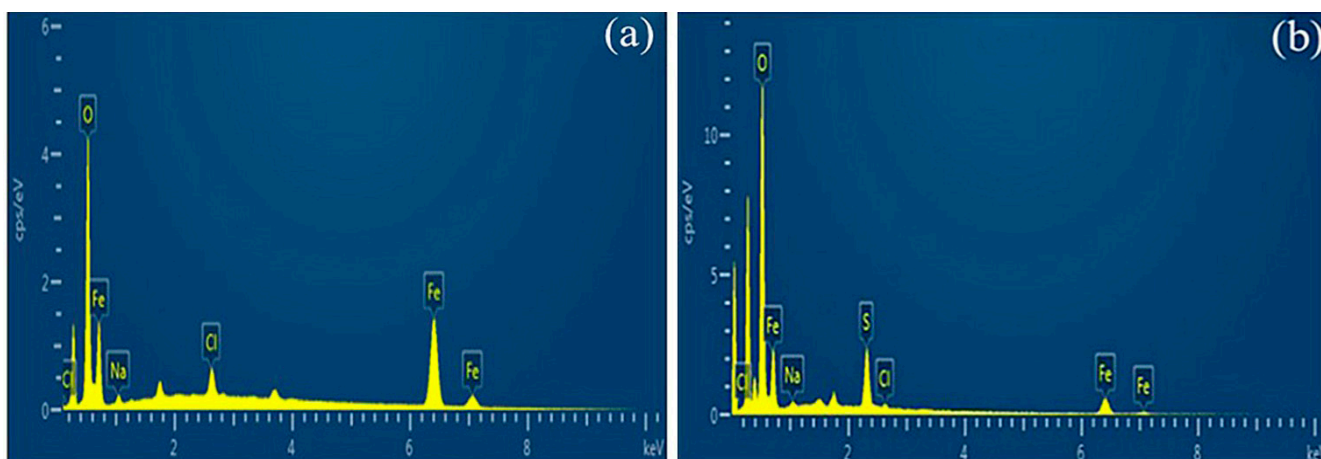


Figure 9. EDS of flocculation product: (a) electroflocculation; (b) electroflocculation with peroxymonosulfate.

Table 3. Element composition and proportion of flocculation products.

Element	Electroflocculation	Electroflocculation with Peroxymonosulfate
O	59.87	63.54
Na	2.44	0.87
S	–	8.91
Cl	0.98	0.72
Fe	36.72	25.96

2.3.5. CV Analysis

The CV results, as presented in Figure 10, reveal significant differences between the electroflocculation method alone and the electroflocculation-peroxymonosulfate combined

treatment. Electroflocculation alone produces only a weak oxidation peak, indicating that the oxidation reaction at the electrode is largely irreversible. In contrast, the shift to a more positive potential in the electroflocculation-persulfate system implies the formation of reactive species, suggesting the generation of strongly oxidizing substances, such as sulfate radicals, which are stronger oxidants than hydroxyl radicals. Furthermore, the significant increase in peak current observed with the addition of peroxydisulfate indicates the enhanced electrical conductivity of the solution, which accelerates the oxidation rate of organic matter.

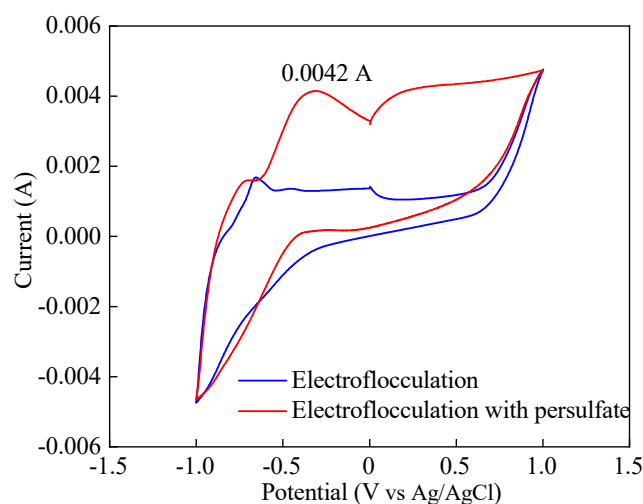


Figure 10. EDS of flocculation product: electroflocculation and electroflocculation with peroxydisulfate.

3. Experimental and Materials

3.1. Materials

All the reagents were analytically pure without any purification. The original shale gas flowback wastewater was taken from a shale gas production base in a pale yellow turbid state in Yibin, Sichuan Province, China. The characteristics and parameters of shale gas flowback wastewater were as shown in Table 4.

Table 4. The characteristics and basic parameters of shale gas flowback wastewater.

Color	COD (mg/L)	TOC (mg/L)	NH ₃ – N (mg/L)	NO ₃ [–] – N (mg/L)	NO ₂ [–] – N (mg/L)	pH	Conductivity (ms/cm)
Light yellow	3799	1312	1688	247	16.4	8.5	26.8

3.2. Experimental Methods

The pure iron electrode (3 cm long, 2 cm wide, 0.3 cm thick) was polished with 2000 mesh sandpaper, immersed in diluted hydrochloric acid for 10 min to remove surface impurities, cleaned ultrasonically, and dried completely. The pure iron electrode served as the anode, while a titanium plate (7 cm long, 1 cm wide, 0.3 cm thick) functioned as the cathode. A volume of 500 mL of shale gas flowback wastewater was introduced into the electrolytic cell, and a precision DC power supply was used to optimize the current density. Reaction conditions, such as pH and electrode spacing, were adjusted to enhance the treatment efficiency of the electroflocculation process. The amount of potassium peroxydisulfate added was determined based on the mass change of Fe²⁺ and the reaction formula (1) involving activated peroxydisulfate. Sampling and analysis

were conducted at 5-min intervals to investigate the combined effects of current density, pH (by using 1 M H₂SO₄ or NaOH to adjust the pH to the target value), and KHSO₅ nanoparticle concentration (900~2100 mg/L) on treatment efficiency and explore initial reaction kinetics. The resulting flocculation products were vacuum-dried at 40 °C for 24 h before being prepared for testing. Characterization of these samples provided insights into the reaction mechanism underlying the collaborative wastewater treatment.

3.3. Characterization and Electrochemical Properties

The COD of the wastewater was determined using the oxidation microreflux method both before and after treatment, with the experimental results representing the average values from three tests. The X-ray diffraction (XRD) analysis of the flocculated products was performed using a Shimadzu XRD-7000 diffractometer (Japan) to determine their primary phase structures. The test conditions for XRD were as follows: Cu-K α radiation with a wavelength of 0.154 nm, operated at 40 kV and 40 mA. The scanning range was 10°~80°, with a step size of 0.02° and a scanning rate of 2°/min. The morphology, structure, and chemical composition of the flocculated products were examined using scanning electron microscopy and energy-dispersive spectroscopy (SEM-EDS) with a Nippon Electron JSM-7800F SEM (JEOL Ltd., Tokyo, Japan). Fourier-transform infrared (FT-IR) spectra of the flocculation products were obtained using a Tensor27 Fourier infrared spectrometer (Bruker Optics, Ettlingen, Germany) to identify the main functional groups. The test range selected in this study was 500–4000 cm⁻¹.

Cyclic voltammetry (CV) was used to determine the reversibility of the redox reaction. CV potentiostatic method was adopted in cyclic voltammetry potentiostatic mode by using an electrochemical workstation (CHI660, Chenhua, Shanghai, China). The working electrode was the iron electrode, the counter electrode was the platinum electrode, and the reference electrode was the saturated Ag/AgCl electrode. The scanning rate was 10 mV/s, the scanning range was -1~1 V, with 50 mL shale gas flowback wastewater was mixed with 50 mL 1 mol/L KOH as the electrolyte.

4. Conclusions

In this study, potassium peroxymonosulfate was introduced into an electrolytic setup using iron as the anode and a titanium plate as the cathode to treat shale gas fracturing flowback wastewater. The process involved anodic electrolysis, where the organic contaminants in the wastewater were oxidized and degraded by sulfate radicals generated through the activation of peroxymonosulfate by Fe²⁺. Simultaneously, Fe²⁺ was oxidized to Fe³⁺, which then combined with hydroxide ions in the solution to form Fe(OH)₃, a flocculating agent. This mechanism facilitated both the flocculation and oxidative degradation of the wastewater, achieving a comprehensive treatment approach. The key findings of the study indicated that the combined use of electroflocculation and potassium peroxymonosulfate significantly enhances the treatment efficiency of flowback wastewater. Operational parameters were optimized to a current density of 40 mA/cm², a pH of 7, and a potassium peroxymonosulfate concentration of 1500 mg/L, under which the COD removal efficiency reached an impressive 93.4%. In comparison, the COD removal efficiency with electroflocculation alone was recorded at 82.4%. The phase analysis of the flocculated material confirmed the effective generation of Fe²⁺, which activated the potassium peroxymonosulfate, leading to the production of highly reactive sulfate radicals. Additionally, detecting Fe₂O₃ within the treated material confirmed the oxidation of Fe²⁺ to Fe³⁺. As a result, the sulfate radicals facilitated the degradation of complex organic pollutants in the wastewater, thereby accelerating reaction kinetics and enhancing the overall effectiveness of the treatment process.

Author Contributions: Y.L.: writing—review and editing, writing—original draft, visualization, software, methodology, data curation, conceptualization. L.X.: visualization, writing—review and editing. Q.F.: review and editing, supervision, resources. P.C.-A.: reviewing—editing. M.G.E.-D.: review and editing. X.L.: review and editing, supervision. All authors have read and agreed to the published version of the manuscript.

Funding: This research was financially supported by the Chongqing Natural Science Foundation General Project (No. 2024NSCQ-MSX2181), the Science and Technology Research Program of the Chongqing Education Commission of China (No. KJQN202404705 and No. KJQN202404704), and the Chongqing Natural Science Foundation project (CSTB2024NSCQ-MSX1263).

Data Availability Statement: Dataset available on request from the authors.

Conflicts of Interest: The authors claim that there are no conflicts of interest.

References

1. Feng, Q.; Xu, L.J.; Liu, C.L.; Wang, H.L.; Jiang, Z.; Xie, Z.H.; Liu, Y.L.; Yang, Z.X.; Qin, Y.J. Treatment of shale gas fracturing wastewater using microbial fuel cells: Mixture of aging landfill leachate and traditional aerobic sludge as catholyte. *J. Clean. Prod.* **2020**, *269*, 121776. [[CrossRef](#)]
2. Yang, H.; Diao, H.L.; Zhang, Y.; Xia, S.B. Treatment and novel resource-utilization methods for shale gas oil based drill cuttings—A review. *J. Environ. Manag.* **2022**, *317*, 115462. [[CrossRef](#)] [[PubMed](#)]
3. Wilson, J.M.; Wang, Y.X.; VanBriesen, J.M. Sources of High Total Dissolved Solids to Drinking Water Supply in Southwestern Pennsylvania. *J. Environ. Eng.* **2014**, *140*, B4014003. [[CrossRef](#)]
4. Zhuang, Y.; Zhang, Z.; Zhou, Z.; Chen, M.; Li, J.; Chen, S. Co-treatment of shale-gas produced water and municipal wastewater: Removal of nitrogen in a moving-bed biofilm reactor. *Process Saf. Environ. Prot.* **2019**, *126*, 269–277. [[CrossRef](#)]
5. Sun, Y.; Wang, D.; Tsang, D.C.W.; Wang, L.; Ok, Y.S.; Feng, Y. A critical review of risks, characteristics, and treatment strategies for potentially toxic elements in wastewater from shale gas extraction. *Environ. Int.* **2019**, *125*, 452–469. [[CrossRef](#)]
6. Feng, Q.; Shu, J.; Jiang, Z.; Gamal El-Din, M.; Hao, Y.; Tan, W.; Liu, C.; Xu, L. A novel biochar composite derived from oil-based drill sludge and cuttings: Structural characterization and electrochemical properties. *Environ. Res.* **2023**, *236 Pt 2*, 116757. [[CrossRef](#)] [[PubMed](#)]
7. Tao, Z.; Liu, C.; He, Q.; Chang, H.; Ma, J. Detection and treatment of organic matters in hydraulic fracturing wastewater from shale gas extraction: A critical review. *Sci. Total Environ.* **2022**, *824*, 153887. [[CrossRef](#)] [[PubMed](#)]
8. Yu, Y.; Zhong, Y.W.; Sun, W.L.; Xie, J.J.; Wang, M.Y.; Guo, Z.C. A novel electrocoagulation process with centrifugal electrodes for wastewater treatment: Electrochemical behavior of anode and kinetics of heavy metal removal. *Chemosphere* **2023**, *310*, 136862. [[CrossRef](#)]
9. Seth, K.; Busse, M.; Jang, G.; Joag, S.; Kim, K.; Pankratz, T.; Sahu, D.; Sharma, R.; Stokes-Draut, J.; Tsouris, C.; et al. Electrocoagulation of high-salinity produced water: Lessons learned from its early applications in unconventional reservoir plays. *Curr. Opin. Chem. Eng.* **2023**, *42*, 100952. [[CrossRef](#)]
10. Shahedi, A.; Darban, A.K.; Jamshidi-Zanjani, A.; Homae, M. An overview of the application of electrocoagulation for mine wastewater treatment. *Environ. Monit. Assess.* **2023**, *195*, 522. [[CrossRef](#)]
11. An, C.J.; Huang, G.; Yao, Y.; Zhao, S. Emerging usage of electrocoagulation technology for oil removal from wastewater: A review. *Sci. Total Environ.* **2017**, *579*, 537–556. [[CrossRef](#)]
12. Kausley, S.B.; Malhotra, C.P.; Pandit, A.B. Treatment and reuse of shale gas wastewater: Electrocoagulation system for enhanced removal of organic contamination and scale causing divalent cations. *J. Water Process Eng.* **2017**, *16*, 149–162. [[CrossRef](#)]
13. Gao, X.; Li, P.; Wang, X.; Guo, Y.; Liao, P.; Liu, Z.; Fan, H. Comparison of treatment efficiency of uranium (VI) containing wastewater using flocculation and electrocoagulation processes. *Chin. J. Environ. Eng.* **2018**, *12*, 488–496.
14. Franco, D.; Lee, J.; Arbelaez, S.; Cohen, N.; Kim, J.Y. Removal of phosphate from surface and wastewater via electrocoagulation. *Ecol. Eng.* **2017**, *108*, 589–596. [[CrossRef](#)]
15. Verma, A.K. Treatment of textile wastewaters by electrocoagulation employing Fe-Al composite electrode. *J. Water Process Eng.* **2017**, *20*, 168–172. [[CrossRef](#)]
16. Ma, W.; Ye, Y.; Chen, S.; Zhao, H.; Liu, G. Treatment of drilling wastewater in polysulfonic slurry system by electric flocculation. *Environ. Prot. Chem. Ind.* **2004**, *z1*, 196–198.
17. Wang, Z.; Song, B.; Li, J.; Teng, X. Degradation of norfloxacin wastewater using kaolin/steel slag particle electrodes: Performance, mechanism and pathway. *Chemosphere* **2021**, *270*, 128652. [[CrossRef](#)] [[PubMed](#)]
18. Mohamed Awad Fagier, M.S.; Mona, O. Abdalrhman, Combination of Persulfate /Peroxymonosulfate Activated By Ion (II) with Hydrogen Peroxide for Mineralization and Valorization of Vinasse. *Biointerface Res. Appl. Chem.* **2020**, *11*, 7519–7527.

19. Jorge, N.; Teixeira, A.R.; Gomes, A.; Lucas, M.S.; Peres, J.A. Sulfate Radical Advanced Oxidation Processes: Activation Methods and Application to Industrial Wastewater Treatment. In Proceedings of the 4th International Electronic Conference on Applied Sciences, online, 27 October–10 November 2023.
20. Li, J.; Ren, Y.; Lai, L.D.; Lai, B. Electrolysis assisted persulfate with annular iron sheet as anode for the enhanced degradation of 2, 4-dinitrophenol in aqueous solution. *J. Hazard. Mater.* **2018**, *344*, 778–787. [[CrossRef](#)]
21. Zhu, L.; Huang, D.K.; Du, H. Pretreatment of Rubber Additives Processing Wastewater by Aluminum-Carbon Micro-Electrolysis Process: Process Optimization and Mechanism Analysis. *Water* **2022**, *14*, 582. [[CrossRef](#)]
22. Nidheesh, P.V.; Murshid, A.; Chanikya, P. Combination of electrochemically activated persulfate process and electro-coagulation for the treatment of municipal landfill leachate with low biodegradability. *Chemosphere* **2023**, *338*, 139449. [[CrossRef](#)]
23. Guan, Y.-H.; Ma, J.; Li, X.-C.; Fang, J.-Y.; Chen, L.W. Influence of pH on the formation of sulfate and hydroxyl radicals in the UV/peroxymonosulfate system. *Environ. Sci. Technol.* **2011**, *45*, 9308–9314. [[CrossRef](#)] [[PubMed](#)]
24. Zhan, H.; Liu, X.; Huang, J.; Liu, X.; Zhang, X.; Yao, J.; Xie, S. Iron electrocoagulation activated peracetic acid for efficient degradation of sulfamethoxazole. *Chem. Eng. Res. Des.* **2023**, *200*, 244–255. [[CrossRef](#)]
25. Akkaya, G.K. Treatment of petroleum wastewater by electrocoagulation using scrap perforated (Fe-anode) and plate (Al and Fe-cathode) metals: Optimization of operating parameters by RSM. *Chem. Eng. Res. Des.* **2022**, *187*, 261–275. [[CrossRef](#)]
26. Gatsios, E.; Hahladakis, J.N.; Gidaracos, E. Optimization of electrocoagulation (EC) process for the purification of a real industrial wastewater from toxic metals. *J. Environ. Manag.* **2015**, *154*, 117–127. [[CrossRef](#)]
27. Ghanbari, F.; Wu, J.; Khatebasreh, M.; Ding, D.; Lin, K.-Y.A. Efficient treatment for landfill leachate through sequential electrocoagulation, electrooxidation and PMS/UV/CuFe₂O₄ process. *Sep. Purif. Technol.* **2020**, *242*, 116828. [[CrossRef](#)]
28. Ismail, L.; Ferronato, C.; Fine, L.; Jaber, F.; Chovelon, J.-M. Elimination of sulfaclozine from water with SO₄⁻ radicals: Evaluation of different persulfate activation methods. *Appl. Catal. B Environ.* **2017**, *201*, 573–581. [[CrossRef](#)]
29. Balti, I.; Smiri, L.S.; Rabu, P.; Gautron, E.; Viana, B.; Jouini, N. Synthesis and characterization of rod-like ZnO decorated with γ-Fe₂O₃ nanoparticles monolayer. *J. Alloys Compd.* **2014**, *586*, S476–S482. [[CrossRef](#)]
30. Singh, S.P.; Park, W.B.; Yoon, C.; Kim, D.; Sohn, K.-S. Combinatorial Screening of Eu²⁺ and Ce³⁺-doped AE-Sc-Si-O-N (AE = Mg, Ca, Sr, Ba) System and Discovery of a Phosphor for White Light Emitting Diode. *ECS J. Solid State Sci. Technol.* **2015**, *5*, R3032–R3039. [[CrossRef](#)]
31. Sibiya, N.P.; Rathilal, S.; Tetteh, E.K. Coagulation Treatment of Wastewater: Kinetics and Natural Coagulant Evaluation. *Molecules* **2021**, *26*, 698. [[CrossRef](#)] [[PubMed](#)]
32. Zhou, Y.; Wu, L.; Li, Y.; Bai, J. Analysis of synthesis structures and flocculation stability of a polyphosphate ferric sulfate solid. *Chem. Eng. J. Adv.* **2022**, *9*, 100202. [[CrossRef](#)]

Disclaimer/Publisher’s Note: The statements, opinions and data contained in all publications are solely those of the individual author(s) and contributor(s) and not of MDPI and/or the editor(s). MDPI and/or the editor(s) disclaim responsibility for any injury to people or property resulting from any ideas, methods, instructions or products referred to in the content.